

# Characterizing a Fabry-Perot Transfer Cavity

Charles Gaomi Zha  
Advisor: Dr. Thomas Killian  
Rice University

April 24, 2013

# Contents

<b>1</b>	<b>Introduction</b>	<b>3</b>
1.1	Motivation . . . . .	3
1.2	Background . . . . .	3
1.2.1	Gaussian Beams . . . . .	3
1.2.2	Fabry-Perot Cavity . . . . .	4
1.2.3	Mode Matching . . . . .	5
<b>2</b>	<b>Characterizing the Cavity</b>	<b>6</b>
2.1	Experimental Setup . . . . .	6
2.2	The Cavity . . . . .	6
2.3	Beam Profiling . . . . .	7
2.4	Mode Matching . . . . .	8
2.5	Alignment . . . . .	10
2.6	Measurements . . . . .	10
<b>3</b>	<b>Results</b>	<b>11</b>
<b>4</b>	<b>Improving the Cavity</b>	<b>11</b>
4.1	Increasing Scanning Range . . . . .	13
4.2	Replacing Mirrors . . . . .	13
<b>5</b>	<b>Conclusion</b>	<b>14</b>

# 1 Introduction

## 1.1 Motivation

The laser is an important tool in the study of ultracold phenomenon. It facilitates basic tasks such as trapping and cooling of atoms in a magnet-optical trap [6], exciting electrons to specific energy states, and creation of neutral ultracold plasmas by photoionization [2]. Because these lasers operate on specific energy state transitions, they must have a stable output frequency tuned precisely to the desired energy level difference, and an external locking mechanism is often required.

When an existing master laser has already been stabilized, additional slave lasers can be stabilized using a transfer Fabry-Perot cavity: The length of the cavity is first locked to the master laser, then the slave laser is locked to the cavity. [7]

An upcoming experiment at the Killian research lab requires a stable 640 nm laser. The goal of this project is to characterize a Fabry-Perot cavity, which will be used as a transfer cavity to lock the new 640 nm laser to an existing 689 nm laser. Experimental data will be compared to theoretical expectations to ensure the validity of observation.

## 1.2 Background

### 1.2.1 Gaussian Beams

Ray optics, which model light as rays traveling in straight lines, is not sufficient to describe how laser beams propagate in free space; its wave nature must be taken into account.

Modeling the laser beam as a plane wave with a slowly varying complex amplitude and solving the wave equation, the simplest solution describes a Gaussian beam [4], often called the “fundamental mode”. In the transverse direction, the beam has a Gaussian amplitude profile, and in the longitudinal direction a hyperbolic profile.

For a given wavelength  $\lambda$ , the properties of a beam along its direction of propagation (denoted as the  $z$ -axis) can be characterized by a single complex parameter  $q(z)$ . The parameter at different positions along the beam satisfies  $q(z_1 + d) = q(z_1) + d$ .

For convenience, two real beam parameters  $R$  and  $w$  can be introduced:

$$\frac{1}{q} = \frac{1}{R} - j \frac{\lambda}{\pi w^2} \tag{1}$$

$R(z)$  represents the radius of curvature of the wavefront at  $z$ , and  $w$  represents the beam radius, the distance from the axis where the amplitude of the electric field drops to  $1/e$  times that on the axis.

At the *beam waist*,  $q$  is purely imaginary, and the beam radius attains its minimum value  $w_0$ . Putting the beam waist at  $z = 0$ , the beam parameter  $q$  at any  $z$  is given by:

$$q(z) = j \frac{\pi w_0^2}{\lambda} + z \tag{2}$$

Combining (1) and (2) gives an expression for the beam radius at any position in terms of the waist radius:

$$w^2(z) = w_0^2 \left[ 1 + \left( \frac{\lambda z}{\pi w_0^2} \right)^2 \right] \quad (3)$$

The transformation of Gaussian beams by optical elements such as lenses can be expressed in terms of the same  $ABCD$  ray transfer matrix used in ray optics, but the transformation rule is different. The  $ABCD$  matrix for vacuum of length  $d$  is  $\begin{pmatrix} A & B \\ C & D \end{pmatrix} = \begin{pmatrix} 1 & d \\ 0 & 1 \end{pmatrix}$ , and that of a thin lens of focal length  $f$  is  $\begin{pmatrix} 1 & 0 \\ -\frac{1}{f} & 1 \end{pmatrix}$ ; check [4] or an optics book for a complete listing for common optical elements. For a given optical element, the beam parameter just after the element is related to that just before it by:

$$q_2 = \frac{Aq_1 + B}{Cq_1 + D} \quad (4)$$

Apart from the fundamental mode, there are higher order modes of propagation, which share the same longitudinal profile but have different transverse modes. In Cartesian coordinates, they are represented as Hermite-Gaussian modes and denoted as  $TEM_{mn}$ , where  $m$  and  $n$  denote the number of nodes (area of zero intensity) in each Cartesian direction. Therefore,  $TEM_{00}$  has no nodes in its transverse profile and denote the fundamental mode, where  $TEM_{12}$  has 1 node in one Cartesian direction and 2 nodes in the other.

The modes can also be represented in cylindrical coordinates as Laguerre-Gaussian modes. Both representations form complete and orthogonal sets of basis functions, and representation in one can be converted to the other [3].

### 1.2.2 Fabry-Perot Cavity

A Fabry-Perot cavity consists of two mirrors facing each other. If the cavity is stable, Gaussian beams having certain parameters can resonate in it, i.e. the beam parameter is the same after it completes a complete round-trip. From this condition, the requirements for a laser beam to resonate can be derived [4]. The cavity used in this project is one with concave mirrors of equal curvature, so only this case is detailed below.

For a cavity with concave mirrors of equal radius of curvature  $R$  and spacing  $d$  between the mirrors, the free spectral range (FSR), the spacing between successive resonances in frequency, for on-axis light is given by

$$\nu_0 = c/2d \quad (5)$$

and the resonant frequencies are given by

$$\nu/\nu_0 = (q + 1) + \frac{1}{\pi} (m + n + 1) \arccos(1 - d/R) \quad (6)$$

where  $q$  is the number of longitudinal nodes in the standing wave (therefore a large non-negative integer), and  $m, n$  are the mode numbers for Hermite-Gaussian modes.

Inside the cavity, the radius of the beam waist is given by

$$w_0^2 = \frac{\lambda}{2\pi} \sqrt{d(2R - d)} \quad (7)$$

and the waist is located exactly midway between the two mirrors for this symmetric cavity.

The finesse of the cavity is the ratio of the free spectral range to the cavity bandwidth, i.e. the FWHM of the resonance transmission peaks. [8] It expresses the resolving power of the cavity.

Fabry-Perot cavities often have mechanisms to fine-tune the length of the cavity, therefore shifting (“scanning”) the resonant frequencies. Since the scanning range is usually the order of wavelengths, the change in  $d$  is very small, and the right-hand side of (6) can be treated as constant. Therefore  $\nu$  scales linearly with  $\nu_0$ , i.e. the resonant wavelengths scale linearly with  $d$ .

### 1.2.3 Mode Matching

Only light that matches the parameters given in the preceding section resonates inside a cavity and transmits through; light that does not match is reflected. In order to couple as much light into the cavity as possible, the incoming laser beam must have parameters matching those of a resonating mode. The process of modifying the parameters of a laser beam to match that of a cavity is called mode matching.

A thin lens is often used for this purpose, and the appropriate lens to use can be determined by the process below [4]. For convenience, we introduce the confocal parameter  $b$  of a beam, defined in terms of the waist radius and wavelength:

$$b = \frac{2\pi w_0^2}{\lambda} \quad (8)$$

To match two beams with confocal parameters  $b_1$  and  $b_2$ , a thin lens with focal length  $f > f_0$  can be used, where  $f_0^2 = \frac{1}{4}b_1b_2$ . Then the distances between the lens and beam waists are

$$\begin{aligned} d_1 &= f \pm \frac{1}{2}b_1 \sqrt{\frac{f^2}{f_0^2} - 1} \\ d_2 &= f \pm \frac{1}{2}b_2 \sqrt{\frac{f^2}{f_0^2} - 1} \end{aligned} \quad (9)$$

All optical elements on the beam path that may modify the beam must be taken into consideration. The mirrors installed on the Fabry-Perot cavity in this project are plano-concave optical plates with a reflective surface deposited on the concave side. Therefore, the

mirrors act as concave lenses when the beam pass through them. Taking into consideration the thin-lens effect (but not the thickness of the lens), the waist radius  $w_0$  and position from entry mirror  $t$ , as seen from the outside, is given by [4]

$$\begin{aligned}\frac{1}{2}b &= \frac{R\sqrt{d(2R-d)}}{2R+d(n^2-1)} \\ t &= \frac{ndR}{2R+d(n^2-1)}\end{aligned}\tag{10}$$

where  $n$  is the refractive index of the mirror's substrate.

## 2 Characterizing the Cavity

### 2.1 Experimental Setup

See Figure 1 for the layout of the optical table and relevant equipment. At the beginning of the project, only elements 1 through 6 are installed; the other elements are added later in the project. A laser beam from the stable 689 nm laser emerges from optical fiber 1, passes through lenses 2 and 3 and AOM 4. The zeroth-order beam from the AOM is then picked up by mirrors 5 and 6 and sent rightwards. The origin  $z = 0$  for all further measurements is arbitrarily selected to be the edge of a base plate. The physical path length between the output coupler of fiber 1 and the origin is  $(84.7 \pm 0.2)$  cm.

### 2.2 The Cavity

The Fabry-Perot Cavity used in this project is the side-product of an earlier project. See Figure 2.

The body of the cavity is a solid Invar rod of diameter 5.6 cm and length 19.6 cm, with a hole 0.7 cm in diameter bored through the axis. At each end of the body is a stack of one washer-shaped PZT, one copper washer electrode, another PZT, the mirror, and an Invar cap, in that order. The cap is secured to the body with 4 nylon screws.

The mirrors have a diameter of 1.27 cm and a thickness of 6 mm. The inner surface is high reflective and concave, with a radius of curvature of 25 cm. The outer surface is planar. The substrate of the mirrors is fused silica, which has a refractive index  $n = 1.4555$  for 689 nm light [5]. The distance between the two mirrors is 20.0 cm.

The cavity body and the outer surface of the outer PZT are electrically connected to the outer contact of a BNC connector, while the copper electrode is connected to the inner contact. By connecting the BNC connector to a high-voltage source, the voltage is applied across the PZTs and they expand. The nylon screws stretch slightly, allowing the two mirrors to move further apart. This effect is used to scan the cavity.

From Equations 5, 6 and 10, some characteristics of the cavity can be calculated:

- Free spectral range: 749 MHz
- Frequency spacing between different modes:  $\frac{\nu_{m,n}}{\nu_0} = (q + 1) + 0.4359 \times (m + n + 1)$

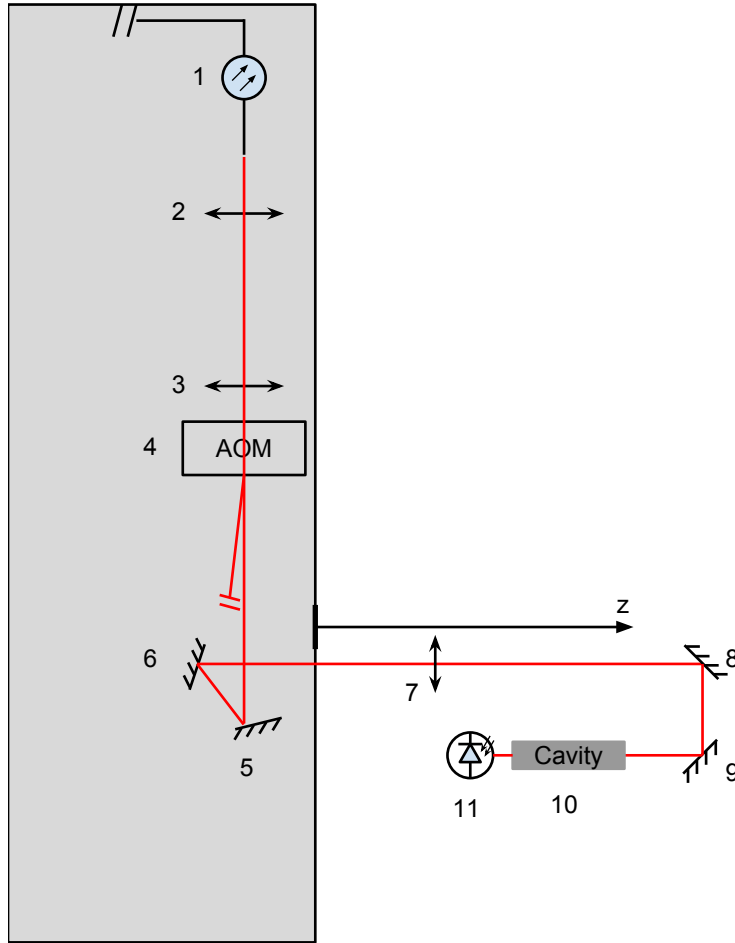


Figure 1: Setup of relevant optical equipment (not to scale)

- Mode-matching properties (virtual beam parameters as seen from outside, taking into consideration lensing and thickness of mirror):
  - Confocal parameter:  $b = 0.1692 \text{ m}$
  - Waist position relative to outer surface of mirror:  $t = 0.1093 \text{ m}$

(Note that strictly, the mode-matching properties are wavelength-dependent, since the refractive index of the mirror substrate is dependent on wavelength.)

### 2.3 Beam Profiling

A commercial beam profiler is used for the measurements in this section. Since the laser beam is slightly elliptic, first the profiler is used to measure the direction of the axes (denoted as V- and W-axis) of the ellipse at several locations along the beam. Pointing the z-axis along the beam and y-axis upwards, the V-axis is at  $-59^\circ$  about the x-axis, and the W-axis

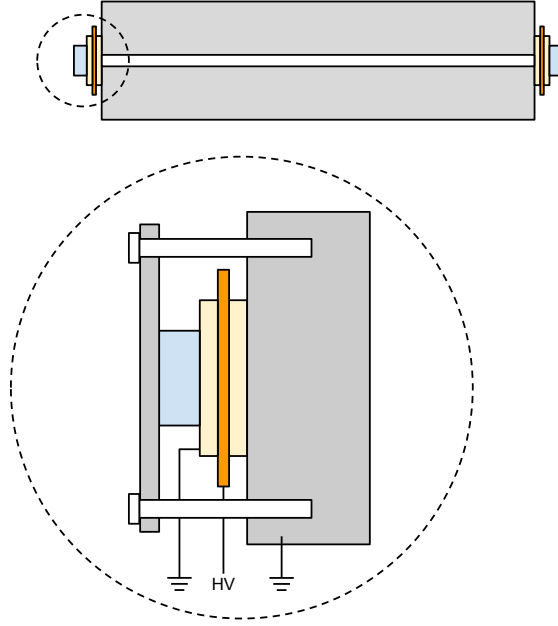


Figure 2: Illustration of the Fabry-Perot cavity used in this project (not to scale)

is at  $+31^\circ$ , estimated to be accurate to  $10^\circ$ . These results are used to adjust the profiler's measuring axes.

Then, the profiler is used to measure the  $1/e^2$  intensity width of the beam on both axes, at several positions along the beam. A best fit for the hyperbolic profile described by (3) is carried out and plotted in Figure 3.

The beam waist on V-axis is located at  $z = (-43.1 \pm 2.1)$  cm with a waist radius  $(0.00896 \pm 0.00028)$  cm, while the waist on W-axis is at  $z = (-43.0 \pm 3.8)$  cm with radius  $(0.0118 \pm 0.0007)$  cm (given with 95% confidence bounds).

Since results on the two axes are close, the beam is treated as spherical, and average values are taken. The beam is characterized by:

- Confocal parameter:  $b = 0.09826$  m
- Waist position:  $z_0 = -0.431$  m

## 2.4 Mode Matching

With knowledge of the beam parameters for both the laser beam and cavity, the optics required for mode matching can now be determined from Equation 9. Considering space available, a lens with design focal length 300 mm is chosen. The actual focal length can be calculated with the lensmaker's equation. The key parameters of the lens are listed below.

- Specifications:
  - Part Number: Thorlabs LA1484-B



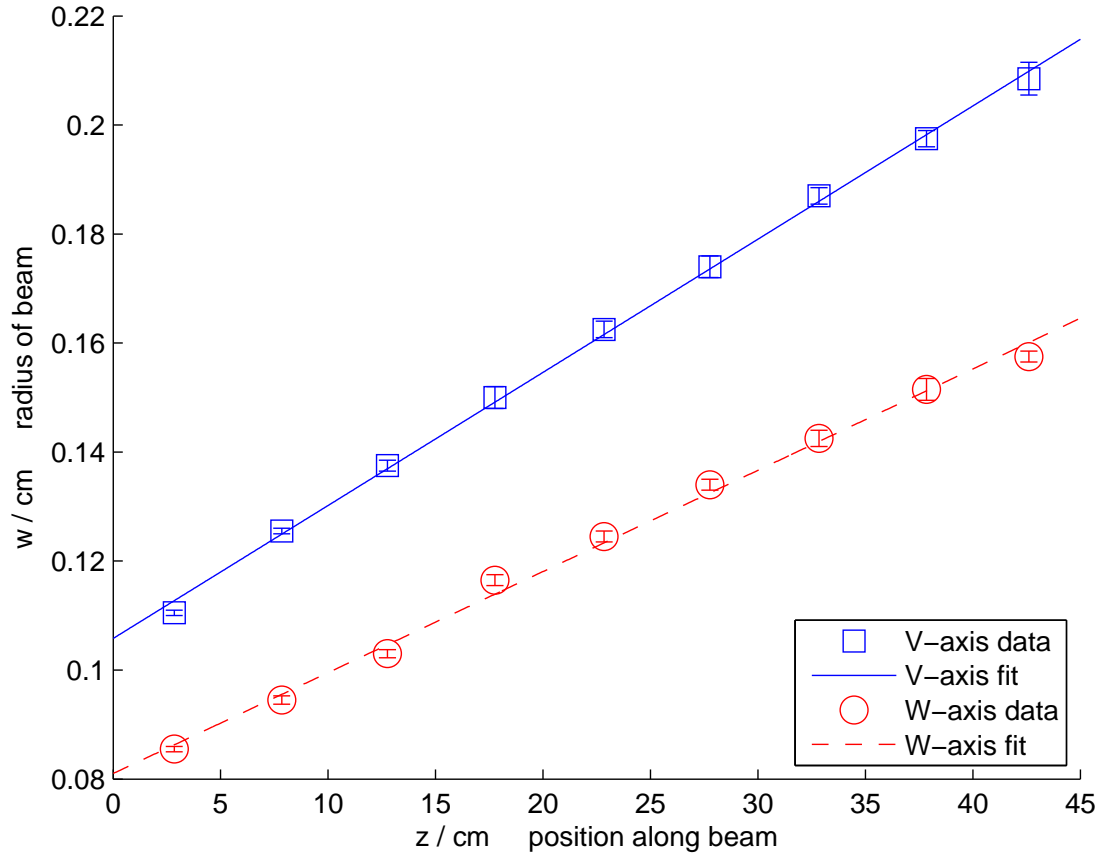


Figure 3: Curve fit for beam width measurements

- Shape: plano-convex
  - Radius of curvature: 154.5 mm
  - Center thickness: 2.5 mm
  - Material: N-BK7
- Refractive index at 689 nm: 1.51336 [1]
  - Focal length at 689 nm: 300.95 mm

The distance between the lens and laser beam's waist is calculated to be 0.52496 m, and the distance between lens and cavity waist is 0.68671 m. The thickness of the lens itself gives a  $-1.28$  mm correction in optical path length. Therefore, the lens should be located at position  $z = 9.4$  cm, and the entry surface of the cavity at  $z = 67.0$  cm.

Refer back to Figure 1. The lens 7, mirrors 8 and 9 and cavity 10 are mounted to the optical table at this step. The two mirrors allow tweaking of both the location and the direction of the beam, which is crucial for the alignment.

## 2.5 Alignment

The goal of alignment is to couple as much energy into the fundamental mode of the cavity as possible.

The sign of a successful alignment is that transmitted power is maximized on resonance. To observe this, scanning the cavity is necessary. A function generator feeds a low frequency (on the order of 10 Hz), 10 V peak-to-peak sawtooth wave into a Thorlabs MDT693A piezo controller, which amplifies the signal to 150 V. The high voltage is then applied to the cavity’s PZTs. A commercial amplified photodetector is placed after the cavity to detect transmission. Both the ramping signal and photodetector output are observed on an oscilloscope.

Rough alignment is done visually: The laser dot is centered on the entry mirror, and normal incidence is achieved by making the reflected beam coincide with the incident beam. At this stage, transmission peaks can be seen on the oscilloscope.

Since there’s no easy way to identify the peak corresponding to the fundamental mode, the next step involves trial and error. Pick a peak and maximize it. If this peak is significantly higher than all others, and if maximizing this peak suppresses the other ones, it is the fundamental mode. Otherwise, pick another peak. Repeat until the fundamental mode is found.

The technique used to maximize a peak is dubbed “walking the beam”. The steps are as follows: Start with either the horizontal or vertical axis. Adjust the near mirror to maximize the peak. Move the far mirror slightly in one direction, and adjust the near mirror to maximize the peak again. If the peak is higher than before, continue moving the far mirror in the same direction, otherwise reverse the direction, and repeat until the far mirror is optimally adjusted. Do the same with the other axis, and repeat as necessary.

## 2.6 Measurements

The same 150 V ramping signal is used to scan the cavity while the height and relative location of every transmission peak is measured. The scanning range does not cover a full FSR, therefore the output frequency of the laser must be shifted in order to survey the entire free spectral range. See Figure 4 for typical oscilloscope screenshots.

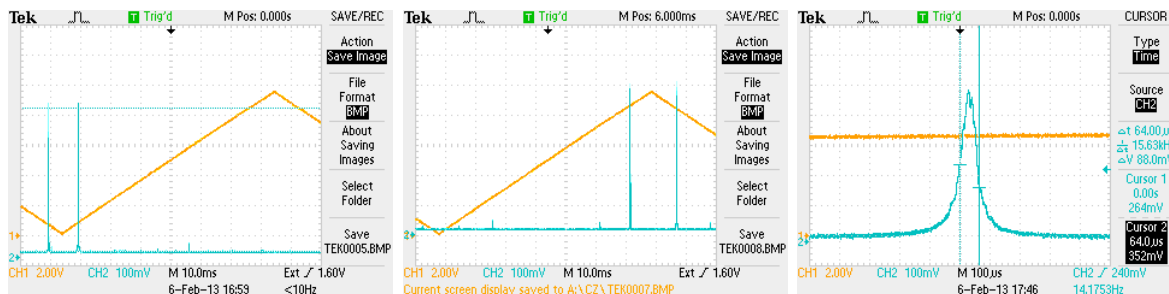


Figure 4: Oscilloscope screenshots

Data from the entire free spectral range is stitched together to produce Figure 5. In Figure 5a, the horizontal scale is the scanning time, and heights of the transmission peaks

are labeled. The free spectral range is 81.3 ms in terms of scanning time, or 164.4 V in terms of PZT ramping voltage. The fundamental mode peak is about 20 times higher than the second highest peak, which is a reasonable result.

In Figure 5b, the horizontal scale is normalized to one FSR, and the relative position of each peak within FSR is labeled. Also, the expected positions of modes are marked. It can be seen that all except 2 peaks are low-order modes that appear at their expected positions. The remaining 2 peaks are likely high-order modes that happen to couple strongly into the cavity.

The FWHM of the fundamental mode peak is 64  $\mu$ s, which corresponds to a finesse of 1270, or a cavity linewidth of 590 MHz.

### 3 Results

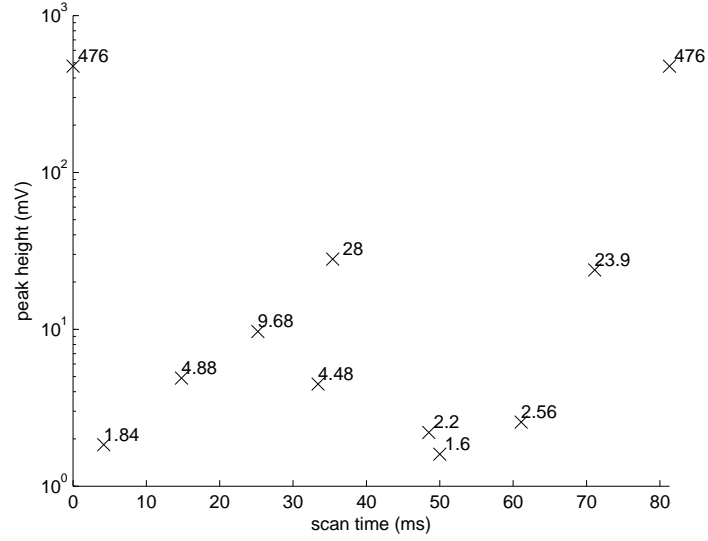
Below is a summary of the characteristics of the Fabry-Perot cavity.

- Length: 20.0 cm
- Mirror radius of curvature: 25 cm
- Free spectral range:
  - In frequency: 749 MHz
  - In PZT ramping voltage: 164.4 V
- Frequency spacing between different modes in terms of FSR: 0.4359
- Finesse: 1270
- Cavity linewidth: 590 kHz
- Mode-matching properties for 689 nm:
  - Confocal parameter:  $b = 0.1692$  m
  - Waist position relative to outer surface of mirror:  $t = 0.1093$  m

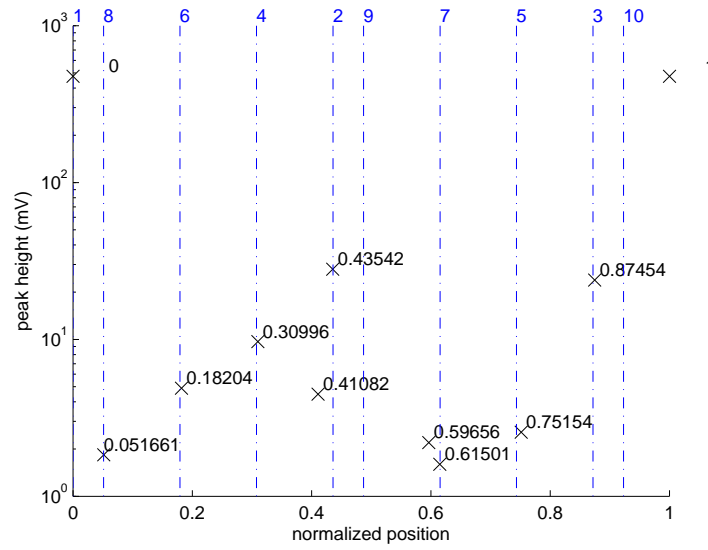
### 4 Improving the Cavity

At this point, a few factors are apparent that make this cavity unsuitable for the intended application - a transfer cavity between a 689 nm and a 640 nm laser - as is. First, the PZTs are unable to scan a full FSR within 150 V, the largest ramping range from piezo controllers we have. This means that in some cases the scanning range will not contain a TEM<sub>00</sub> peak. Second, a higher finesse is desired for an accurate lock. Third, it is discovered that the mirrors used have very low reflectivity at 633 nm - around 70%. Low reflectivity can be expected at 640 nm as well, which means the finesse will be too low for any locking at that wavelength.

Modifications have to be made to remedy these shortcomings.



(a) Peak heights labeled



(b) Relative position within FSR labeled, overlaid with expected positions of modes

Figure 5: Full plots of the free spectral range. Note logarithmic vertical scale.

## 4.1 Increasing Scanning Range

In order to increase the scanning range of the cavity, two additional PZT washers and copper electrodes are installed on one end of the cavity, increasing the number of PZTs on that end to 4. The other end still have 2 PZTs like before.

After the modification, the full FSR can be scanned with a PZT ramping voltage of 107.9 V, less than the maximum range of 150 V of the existing PZT drivers. The separation between mirrors increased to 20.4 cm, which changes the FSR to 735 MHz. The new scanning range is approximately 3/2 times the previous value, which is expected.

## 4.2 Replacing Mirrors

Since the existing mirrors are not adequate for the task, new mirrors have been ordered to replace them. However, the new mirrors will have different physical parameters, which changes many of the cavity characteristics.

The new mirrors will have the following specifications:

- Shape: plano-concave
- Diameter: 1.27 cm
- Thickness: 6 mm
- Radius of curvature: 15 cm
- Substrate: N-BK7
  - Refractive index at 689 nm: 1.51336
  - Refractive index at 633 nm: 1.51508 [1]

Repeating the calculations done in previous sections, the cavity will have the following characteristics once new mirrors are installed:

- Length: 20.4 cm
- Free spectral range:
  - in frequency: 735 MHz
  - in ramping voltage: 107.9 V
- Frequency spacing between modes in terms of FSR: 0.6172
- Mode-matching properties for 689 nm:
  - Confocal parameter: 0.0745 m
  - Waist position relative to entry plane: 0.0913 m
- Mode-matching properties for 633 nm:
  - Confocal parameter: 0.0744 m
  - Waist position relative to entry plane: 0.0913 m

## 5 Conclusion

In conclusion, we have successfully characterized the Fabry-Perot cavity, assessed its suitability as a transfer cavity, and identified and implemented methods to improve it for the purpose.

## References

- [1] Refractive index database. <http://refractiveindex.info/>.
- [2] T. C. Killian, S. Kulin, S. D. Bergeson, L. A. Orozco, C. Orzel, and S. L. Rolston. Creation of an ultracold neutral plasma. *Phys. Rev. Lett.*, 83:4776–4779, Dec 1999.
- [3] Isidoro Kimel and Luis R. Elias. Relations between hermite and laguerre gaussian modes. *Quantum Electronics, IEEE Journal of*, 29(9):2562–2567, 1993.
- [4] H. Kogelnik and T. Li. Laser beams and resonators. *Proceedings of the IEEE*, 54(10):1312–1329, 1966.
- [5] I. H. MALITSON. Interspecimen comparison of the refractive index of fused silica. *J. Opt. Soc. Am.*, 55(10):1205–1208, Oct 1965.
- [6] EL Raab, M. Prentiss, A. Cable, S. Chu, and D.E. Pritchard. Trapping of neutral sodium atoms with radiation pressure. *Physical Review Letters*, 59(23):2631–2634, 1987.
- [7] E. Riedle, S. H. Ashworth, Jr. J. T. Farrell, and D. J. Nesbitt. Stabilization and precise calibration of a continuous-wave difference frequency spectrometer by use of a simple transfer cavity. *Review of Scientific Instruments*, 65(1):42–48, 1994.
- [8] Anthony E. Siegman. *Lasers*. 1986.